ACS APPLIED MATERIALS & INTERFACES

Research Article

www.acsami.org

Microfluidic Templated Mesoporous Silicon–Solid Lipid Microcomposites for Sustained Drug Delivery

Dongfei Liu,[†,⊥] Bárbara Herranz-Blanco,[†,⊥] Ermei Mäkilä,[†,‡] Laura R. Arriaga,[§] Sabiruddin Mirza,[§] David A. Weitz,[§] Niklas Sandler,[∥] Jarno Salonen,[‡] Jouni Hirvonen,[†] and Hélder A. Santos*[,†]

[†]Division of Pharmaceutical Technology, Faculty of Pharmacy, University of Helsinki, FI-00014 Helsinki, Finland

[‡]Laboratory of Industrial Physics, Department of Physics, University of Turku, FI-20014 Turku, Finland

[§]Department of Physics, School of Engineering and Applied Science, Harvard University, Massachusetts 02138, United States

[∥]Pharmaceutical Sciences Laboratory, Department of Biosciences, Åbo Akademi University, FI-20520 Turku, Finland

Supporting Information

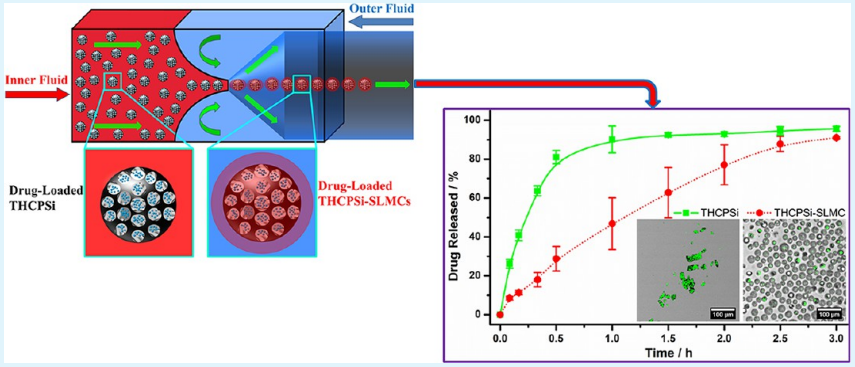

ABSTRACT: A major challenge for a drug-delivery system is to engineer stable drug carriers with excellent biocompatibility, monodisperse size, and controllable release profiles. In this study, we used a microfluidic technique to encapsulate thermally hydrocarbonized porous silicon (THCPSi) microparticles within solid lipid microparticles (SLMs) to overcome the drawbacks accompanied by THCPSi microparticles. Formulation and process factors, such as lipid matrixes, organic solvents, emulsifiers, and methods to evaporate the organic solvents, were all evaluated and optimized to prepare monodisperse stable SLMs. FTIR analysis together with confocal images showed the clear deposition of THCPSi microparticles inside the monodisperse SLM matrix. The formation of monodisperse THCPSi–solid lipid microcomposites (THCPSi–SLMCs) not only altered the surface hydrophobicity and morphology of THCPSi microparticles but also remarkably enhanced their cytocompatibility with intestinal (Caco-2 and HT-29) cancer cells. Regardless of the solubility of the loaded therapeutics (aqueous insoluble, fenofibrate and furosemide; aqueous soluble, methotrexate and ranitidine) and the pH values of the release media (1.2, 5.0, and 7.4), the time for the release of 50% of the payloads from THCPSi–SLMC was at least 1.3 times longer than that from the THCPSi microparticles. The sustained release of both water-soluble and -insoluble drugs together with a reduced burst-release effect from monodisperse THCPSi–SLMC was achieved, indicating the successful encapsulation of THCPSi microparticles into the SLM matrix. The fabricated THCPSi–SLMCs exhibited monodisperse spherical morphology, enhanced cytocompatibility, and prolonged both water-soluble and -insoluble drug release, which makes it an attractive controllable drug-delivery platform.

KEYWORDS: *microfluidics, mesoporous silicon, solid lipid, drug release, microcomposites*

1. INTRODUCTION

Over the past decades, researchers have paid tremendous attention to the development of micro- and nanomaterials-based drug-delivery systems (DDSs).[1−5] The main purpose of using a DDS is to deliver the therapeutics in a spatiotemporal controlled manner: at the desired sites, with the required rate, and for a suitable time period. This control overcomes the adverse physicochemical and biopharmaceutical properties of the drugs and ultimately improves their bioavailability, therapeutic efficacy, and safety.[3−5] However, conventional DDSs often suffer from premature drug release, which results in a sharp increase of drug concentrations to potentially toxic levels. Therefore, the development of advanced DDSs with outstanding biocompatibility, biodegradability, and stability as well as high drug-loading capacity is of tremendous benefit to provide effective and sustained therapy with minimal side effects.[3,4]

Porous silicon (PSi)-based materials have emerged as versatile carriers for drug delivery[5−11] and imaging applications[12−14]

Received: September 14, 2013
Accepted: November 1, 2013
Published: November 1, 2013

because of their attractive properties. These materials have a marked stability as well as biocompatibility. In addition, they have a high-drug-loading capacity because of the large pore volume and surface area available in their pores.[7,14−19] More importantly, PSi degrades to nontoxic silicic acid in vivo, and the degradation rate can be controlled by adjusting the porosity of the material and its surface chemistry.[19−21] Benefiting from these advantages, a wide variety of therapeutic and imaging agents have been successfully loaded into PSi particles by an immersion method.[7] However, owing to the freely accessible pores of PSi, constituents in the body fluid can displace the drugs that are initially loaded within these pores, resulting in premature drug release.[22−24]

To overcome this issue, PSi particles can be encapsulated within a matrix that seals their pores, sustaining the release of the payloads for a much longer time. Recently, we have demonstrated the encapsulation of PSi particles within solid lipid matrices using a solid-in-oil-in-water (S/O/W) emulsion solvent-evaporation method,[25] which retarded the release of the payloads from the PSi nanoparticles. However, this method requires high weight ratios of solid lipid carriers to PSi particles (>200:1) to guarantee the efficient encapsulation of the PSi particles within the solid lipid carrier.[25] Furthermore, centrifugation is needed to sort the components and ultimately to isolate the encapsulated PSi particles,[25,26] which frequently results in caking of the particles. Additionally, the polydispersity and batch-to-batch variation in both the size and morphology of the solid lipid carriers often lead to undesirable variation in the release profiles of the payloads, which ultimately affects the pharmacokinetics of the drugs.[27,28] Moreover, large particles, as those on the upper end of the particle size distribution, promote the formation of aggregates and lead to stability problems.[29] These drawbacks limit the applicability of this drug-delivery system.

Microfluidic technology provides a low-cost and easy-to-use platform for the fabrication of monodisperse droplets. By carefully tuning the flow of several immiscible fluids, monodisperse single-emulsion drops, emulsions containing a single or several inner droplets, topological emulsion drops, Janus particles, microcapsules, microparticles, and even nano-sized carriers are prepared with an exquisite degree of control.[30−35] Because of the wide range of constituent fluids that can be used, droplets of various chemical compositions can be easily prepared. This flexibility in material choice together with the diversity of emulsion order greatly broadens the range of carriers that can be prepared,[28] making microfluidic technologies ideal for the fabrication of advanced DDSs.

In this work, we reported an advanced DDS fabricated by microfluidic technology, which overcame the major drawbacks of DDSs prepared by conventional approaches. Our DDS consisted of mesoporous silicon microparticles (thermally hydrocarbonized porous silicon; THCPSi) encapsulated within a solid lipid matrix (SLM). The resultant microcomposites (THCPSi−SLMCs) were highly monodisperse and had a well-controlled composition and surface chemistry; this significantly enhanced their cytocompatibility in intestinal cancer cells. Furthermore, these microcomposites reduced the undesired burst-release effect, allowing for the sustained release of payloads. We conducted our tests using four model drugs: methotrexate, ranitidine, fenofibrate, and furosemide. These drugs represent a wide range of different physicochemical properties, for instance, different solubilities and lipophilicities. Altogether, our results demonstrated the potential of these microcomposites to encapsulate efficiently and to release controllably either hydrophilic or hydrophobic drugs.

2. EXPERIMENTAL PROCEDURES

2.1. Fabrication and Characterization of THCPSi Microparticles. The preparation and characterization of THCPSi microparticles has been described in detail elsewhere.[13,14,36−38] Briefly, the PSi films were fabricated by electrochemically anodizing monocrystalline, boron-doped, p^+-type Si⟨100⟩ wafers of 0.01 to 0.02 Ω cm resistivity in a 1:1 (v/v) hydrofluoric acid (HF) (38%)/ethanol solution using a current density of 50 mA/cm^2. The film was detached from the Si wafer by abruptly increasing the etching current to the electropolishing region. After the anodization, the free-standing PSi films were ball-milled and dry-sieved on a test sieve with 25 μm openings. The milling and sieving cycles were repeated several times to achieve the desired particle size. The sieved particles were treated with HF/ethanol solution to remove the oxides formed during the milling and dried at 65 °C for 2 h. The hydrogen-terminated microparticles were initially placed under N_2 flow for 30 min before being exposed to acetylene for 15 min at room temperature and at 500 °C under constant flow of N_2 and acetylene (1:1) to obtain thermally hydrocarbonized PSi (THCPSi) microparticles.

The properties of THCPSi microparticles were characterized with N_2 sorption at 77 K using a TriStar 3000 gas sorption apparatus (Micromeritics Inc., Norcross, USA). The specific surface area and pore volume was calculated from the isotherm using the Brunauer−Emmett−Teller theory (BET).[39] The average pore diameter was estimated using the obtained values of specific surface area and the total volume at a relative pressure of $p/p_0 = 0.97$ by assuming the pores to be cylindrical. The calculated values for the THCPSi microparticles provided a specific surface area of 224 ± 3 m^2/g, a pore volume of 0.75 ± 0.01 cm^3/g, and an average pore diameter of 13.4 ± 0.1 nm. The particle size distribution of the THCPSi microparticles after sieving was determined using a Sympatec Helos laser diffractometer equipped with a cuvette wet disperser system (Sympatec GmbH, Clausthal-Zellerfeld, Germany). For the measurement, the microparticles were dispersed into ethanol and stirred at 400 rpm. The mean particle size was determined as ca. 16 μm.

2.2. Fabrication of a Glass-Capillary Microfluidic Flow-Focusing Device. The microfluidic flow-focusing device was made by assembling borosilicate glass capillaries on a glass slide.[40] One end of the cylindrical capillary (World Precision Instruments, Inc.) with inner and outer diameters of around 580 and 1000 μm, respectively, was tapered using a micropipet puller (P-97, Sutter Instrument Co., USA) to a diameter of 20 μm; this diameter was further enlarged to approximately 80 μm using a microforge (P-97, Sutter Instrument Co., USA). This cylindrical tapered capillary was inserted into the left end of the square capillary with inner dimension of around 1000 μm (Vitrocom, USA) and coaxially aligned. A transparent epoxy resin (5 min Epoxi, Devcon) was used to seal the capillaries where required. Two immiscible liquids were injected separately into the microfluidic device through polyethylene tubes attached to syringes at constant flow rates. The flow rate of the different liquids was controlled by pumps (PHD 2000, Harvard Apparatus, USA).

2.3. Preparation of Solid Lipid Microparticles and THCPSi−SLMCs. The solid lipid microparticles (SLM) were prepared by the microfluidic flow-focusing device, as illustrated in Figure 1. In general, the lipid matrix was dissolved in the organic solvents and served as the inner oil fluid. It contained stearic acid (20 mg/mL, w/v) and egg phosphatidylcholine (egg-PC; 40 mg/mL, w/v), which was dissolved in ethyl acetate. Meanwhile, the solution containing amphiphilic Poloxamer 188 (P-188; 1%, w/v), which could efficiently stabilize the O/W interface, was selected as the outer continuous fluid. The inner and outer fluids were separately pumped into the microfluidic flow-focusing devices for preparing the monodispersed O/W emulsions. The inner oil fluid flowed at a typical rate of 2000 μL/h and was focused by the outer continuous fluid, which flowed at a typical rate of 40 000 μL/h (Figure 1). The fabrication was performed at room temperature. For the preparation of THCPSi−SLMCs and drug-loaded THCPSi−SLMCs, bare THCPSi microparticles or drug-loaded THCPSi microparticles

were dispersed into the organic inner fluid (10 mg/mL) under continuous stirring; the preparation procedure was exactly the same as for bare SLMs. All of the collected microparticles or microcomposites were solidified on ice for further characterization.

2.4. Characterization of THCPSi–SLMCs. For the confocal imaging, THCPSi microparticles were first labeled with Rhodamine 123 (Sigma-Aldrich, USA) and then added into the oil fluid to obtain Rhodamine 123-labeled THCPSi–SLMCs. Rhodamine 123-labeled THCPSi microparticles were prepared on the basis of 1-ethyl-3-(3-dimethylaminopropyl)-carbodiimide/*N*-hydroxysuccinimide (EDC/NHS, Thermo Fisher Scientific, USA) conjugation chemistry. First, undecylenic acid-functionalized thermally hydrocarbonized porous silicon (UnTHCPSi)[41] microparticles were activated by addition of excess EDC and NHS for 2 h. Next, the excess amount of Rhodamine 123 ethanol (100 μg/mL) solution was mixed with the activated UnTHCPSi and incubated for 12 h at 25 °C. After centrifugation and washing with ethanol for three times to remove the free Rhodamine 123, Rhodamine 123-labeled THCPSi microparticles were obtained. After organic solvent evaporation, both Rhodamine 123-labeled THCPSi microparticles and THCPSi–SLMCs were separately added onto glass slides and protected by Vectashield mounting medium (Vector Laboratories, USA). Finally, a Leica SP2 inverted confocal microscope (Leica Microsystems, Germany) equipped with argon (488 nm) and DPSS (561 nm) lasers was used to observe the microcomposites. The chemical composition and interaction of the SLM and the PSi microparticles was characterized with a Fourier transformed infrared spectroscopy (FTIR) instrument (Vertex 70, Bruker, USA) using a horizontal attenuated total reflectance (ATR) accessory (MIRacle, PIKE Technologies, USA). The FTIR spectra were recorded at room temperature between 4000–650 cm^{-1} with a resolution of 4 cm^{-1} using OPUS 5.5 software. The zeta-potential distributions were measured by a ZetaSizer Nano-ZS (Malvern Ltd., UK) in water at 25 °C with a folded capillary cell (Malvern Ltd., UK).

2.5. Cell Viability Assay. For the cell viability measurements, mucus-secreting intestinal HT-29 (5.0×10^5 cells/mL) and Caco-2 (2.5×10^5 cells/mL) cells were selected. A suspension of cells in Dulbecco's modified Eagle medium (DMEM) was seeded into 96-well plates (100 μL/well, PerkinElmer Inc., USA) and allowed to attach overnight. After removing the medium and washing the wells twice with fresh 1× Hanks balanced salt solution (HBSS, pH 7.4), the THCPSi microparticle and THCPSi–SLMC suspensions at concentrations of 2000, 1000, 500, 250, and 10 μg/mL were added into the wells (100 μL/well). Positive and negative controls of 1× HBSS (pH 7.4) and Triton X-100, respectively, were used. After 3 and 24 h incubation, the wells were washed once with 1× HBSS (pH 7.4), and the number of viable cells was assayed with CellTiter-Glo (Promega Corporation, USA) according to the manufacturer's instructions. The luminescence was measured on a Varioskan Flash fluorometer (Thermo Fisher Scientific, USA). All of the experiments were performed at least in triplicate.

2.6. Drug Loading and Loading Degree Determination. Different drugs were loaded into THCPSi microparticles using an immersion method.[25,36,42] For all of the four drugs tested, a drug concentration of 30 mg/mL at a ratio of 3:1 (drug/THCPSi particles) and a loading time of 2 h were used. Methotrexate was dissolved in phosphate buffer (pH 8.0), ranitidine was dissolved in ethanol solution (50:50, v/v), and furosemide and fenofibrate were both dissolved in acetone. After loading, all suspensions were ultracentrifuged at 10 000 rpm (5415D, Eppendorf, Germany) for 3 min to remove the excess of free drugs. For the determination of the loading degree of the THCPSi–SLMCs, the drug-loaded THCPSi microparticles were first dispersed into the inner oil fluid under stirring to form the THCPSi–SLMCs with the microfluidic flow-focusing device. Then, the drug-loaded THCPSi microparticles or THCPSi–SLMCs were immersed into a mixture of water and acetone (50:50, v/v) for 24 h, and the amount of drug was determined by the corresponding HPLC method (see Table S1).

2.7. In Vitro Release Tests. For the drug-release tests, the microfluidic system ran for 3 min (representing 100 μL of ethyl acetate solution and 1000 μg of THCPSi microparticles). The collected emulsions were immediately put into a 60 °C water bath to remove the organic solvents followed by the drug-release test. The in vitro drug-release profiles of the four model drugs from drug powders, THCPSi microparticles, and THCPSi–SLMCs were all made in a dialysis bag. First, ca. 100 μg of drug powder, drug-loaded THCPSi microparticles (ca. 1000 μg), and drug-loaded THCPSi–SLMCs (containing ca. 1000 μg of drug-loaded THCPSi microparticles) was added into the dialysis diffusion bags (Spectra/Por, MWCO 1 MDa, Spectrum Laboratories Inc., USA). The drug-release profiles were determined by immersing the dialysis diffusion bag in 25 mL of buffer solutions at different pH values (1.2, 5.0, and 7.4) using a shaking method at 100 rpm and 37 ± 1 °C. Owing to the low solubility of fenofibrate at all of the tested pH values and furosemide at pH 1.2, Tween 80 (1%, w/v) was added into the corresponding release medium during the release test. For each test, samples of 200 μL were withdrawn at different time points, and the same volume of preheated medium was added back to replace the withdrawn volume. After sampling, the concentration of drugs was quantified by HPLC, as described in Table S1.

2.8. Statistical Analyses. Results from several tests are expressed as the mean ± SD for at least three independent experiments. A one-way analysis of variance (ANOVA) followed by the Student's *t*-test was employed to analyze the data. The analysis was carried out using SPSS20 (IBM Corp., USA), and the level of significance was set at a probability of $*p < 0.05$, $**p < 0.01$, and $***p < 0.001$.

3. RESULTS AND DISCUSSION

3.1. Fabrication and Characterization of the Microcomposites. We used oil-in-water (O/W) single-emulsion drops, fabricated by a glass-capillary microfluidic device, as templates for the microcomposites. The device was composed of a square capillary and a cylindrical tapered capillary, as illustrated schematically in Figure 1. The outer diameter of the cylindrical tapered capillary fit the inner dimensions of the square capillary, facilitating the alignment of their axes. The inner fluid was injected into the left extreme of the square capillary, whereas the outer fluid was injected through the interstices between the right end of the square capillary and the cylindrical capillary in the opposite direction. This flow-focusing geometry forced the inner fluid to break up, forming single O/W emulsion drops at the

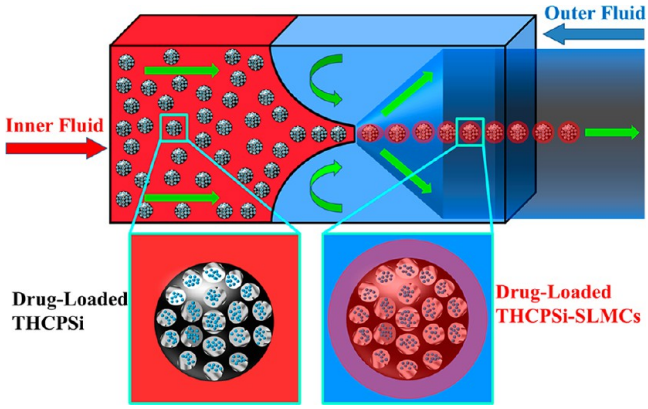

Figure 1. Schematic illustration of the procedure used to prepare monodisperse SLMs and THCPSi–SLMCs (not to scale). The inner fluid consisted of a mixture of lipids (stearic acid, 20 mg/mL; egg phosphatidylcholine, 40 mg/mL) in ethyl acetate that ultimately formed the SLMs. For the preparation of THCPSi–SLMCs, the THCPSi microparticles (10 mg/mL) were dispersed in this inner fluid. The outer continuous fluid was an aqueous solution containing amphiphilic Poloxamer 188 (P-188; 1%, w/v), which could efficiently stabilize the O/W interface. The inner fluid flowed at a typical rate of 2000 μL/h and was focused by the outer continuous fluid, which flowed at a typical rate of 40 000 μL/h. The fabrication was performed at room temperature.

orifice of the cylindrical capillary. We optimized the composition of the templates to provide the resultant microcomposites with maximum stability and biocompatibility. We also investigated different methods to remove the organic solvent efficiently while maintaining the stability of the templates. Details on the formulation optimization and the processes tested to remove the organic solvent are given in the Supporting Information (Figures S1, S2, and S3).

Fluorescently labeled PSi microparticles (Rhodamine 123-labeled PSi microparticles) with irregular shapes, as shown in the top panel of Figure 2a, were used to study the encapsulation

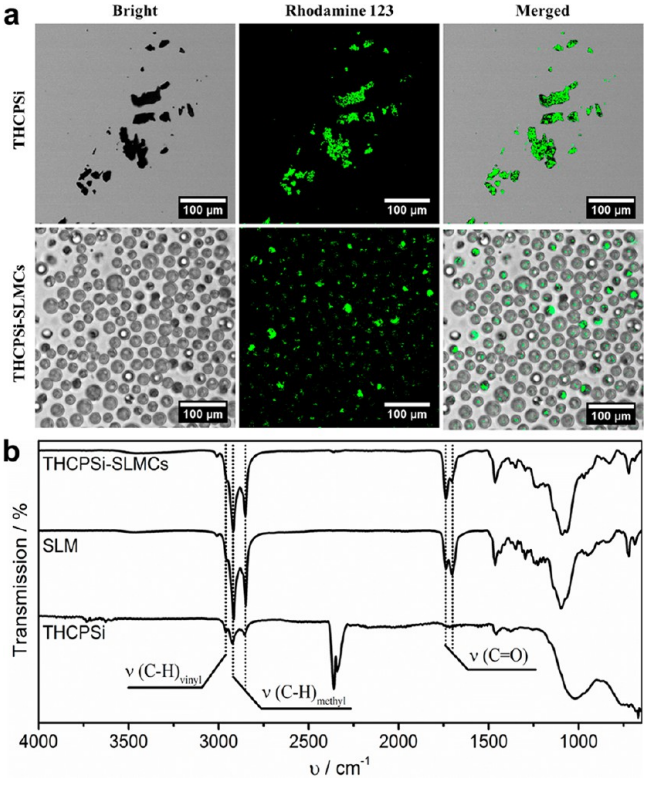

Figure 2. (a) Bright-field and confocal fluorescence images of Rhodamine 123-labeled (green) THCPSi microparticles and THCPSi–SLMCs. (b) ATR–FTIR spectra of the THCPSi microparticles, SLMs, and THCPSi–SLMCs.

ability of the SLMs. The average particle size of PSi microparticles in an ethanol dispersion measured by a laser diffractometer was around 16 μm; however, when we dispersed them in aqueous medium (top panel of Figure 2a), their size looked larger. This phenomenon could be ascribed to the poor dispersibility of PSi microparticles in aqueous medium and their tendency to aggregate as a result of their hydrophobic surface.[25] These Rhodamine 123-labeled PSi microparticles were efficiently encapsulated within the formed SLMs, as shown in the bottom panel of Figure 2a. The obtained spherical-shaped microcomposites had a typical diameter of about 24.9 μm with a variation coefficient of approximately 15.4%; these microcomposites were around 17.8% smaller than the droplets used as templates as a result of the solvent-evaporation process. Importantly, the microcomposites showed outstanding dispersibility; the SLMs reduced the surface hydrophobicity of the bare PSi particles. Diffuse reflectance is a very effective technique in the analysis of powders or whenever the roughness of the analyte surface is not negligible for the incident radiation wavelength. The THCPSi–SLMCs were further characterized by the FTIR, for which a horizontal ATR accessory was adopted to detect the transmission features on the surfaces of the powder (Figure 2b). The FTIR spectrum of the microcomposites was very similar to that of the bare SLMs, and no peak from PSi particles could be detected, which could probably be ascribed to the encapsulation of PSi particles, meaning that the PSi particles were located inside the lipid matrix and thus their signals could not be detected.

3.1.2. In Vitro Viability Experiments. Owing to their micrometric size, these vehicles were envisaged to be applied for oral drug delivery and thus we evaluated their cytocompatibility with gastrointestinal tract (GIT)-related cancer cell lines (Caco-2 and HT-29) by an ATP-based luminescence assay.[43] For the Caco-2 cells, we observed a decrease in the cell viability from approximately 90 to 50% as the dose of PSi microparticles increased from 100 to 2000 μg/mL after 4 h incubation, as shown in Figure 3a. When the incubation time was extended to 24 h, a similar, but more pronounced, result was obtained, as shown in Figure 3b. By contrast, HT-29 cells only showed a weak particle-dose-dependent viability toward the bare PSi microparticles after 4 and 24 h incubation, as shown in Figure 3c,d. After encapsulation of the PSi microparticles within the SLM, the viability of the two cell lines was enhanced significantly. The viability of cells improved further for the higher doses of particles tested (2000 and 1000 μg/mL), particularly for the Caco-2 cells. In the case of Caco-2 cells incubated with particles for 24 h, after encapsulation within SLMs the viability of Caco-2 cells increased from approximately 90 to 100% for the particle concentration of 100 μg/mL, whereas the cell viability increased from approximately 35 to 80% for the particle concentration of 2000 μg/mL.

The cytotoxicity induced by microparticles was a result of their interactions with the membranes of the cells and was mainly determined by the nature of the surface of the particles.[25,44−47] Because of the similar zeta potential that we measured for both the bare PSi microparticles (ca. −35 mV) and the microcomposites (ca. −43 mV), the difference in cell viability that we found cannot be attributed to their surface charge properties. The lower cell viability introduced by the bare PSi microparticles may be due to their stronger hydrophobic interactions with cell membranes,[25,36,43] mainly caused by the inherent hydrophobic nature of THCPSi microparticles and their irregular shapes. In contrast, importantly, the presence of SLMs made the microcomposite more cytocompatible. This is likely due to the higher hydrophilicity and spherical morphology of the microcomposites as compared to the bare irregular-shaped hydrophobic THCPSi microparticles, which probably resulted in a decrease in the interactions between the cells and the microcomposites.[48] The formed large PSi aggregates in aqueous medium, because of their hydrophobic surface,[43] can also contribute to the reduced cell viability observed for the bare PSi particles.

3.1.3. Drug Loading and Release Tests. To evaluate the loading capacity of the microcomposites and their potential to retard the release of payloads, we selected four model drugs with different solubilities in aqueous medium: fenofibrate and furosemide, which are poorly aqueous-soluble, and methotrexate and ranitidine, which are more soluble, as detailed in Table S2 of the Supporting Information. The surface properties of the PSi particles, the chemical structures of the drugs, and the loading media all play critical roles in the loading process.[49] To achieve the highest possible loading of drugs, fenofibrate and furosemide were loaded using acetone as a loading solution, methotrexate was loaded using phosphate buffer (pH 8.0), and ranitidine was

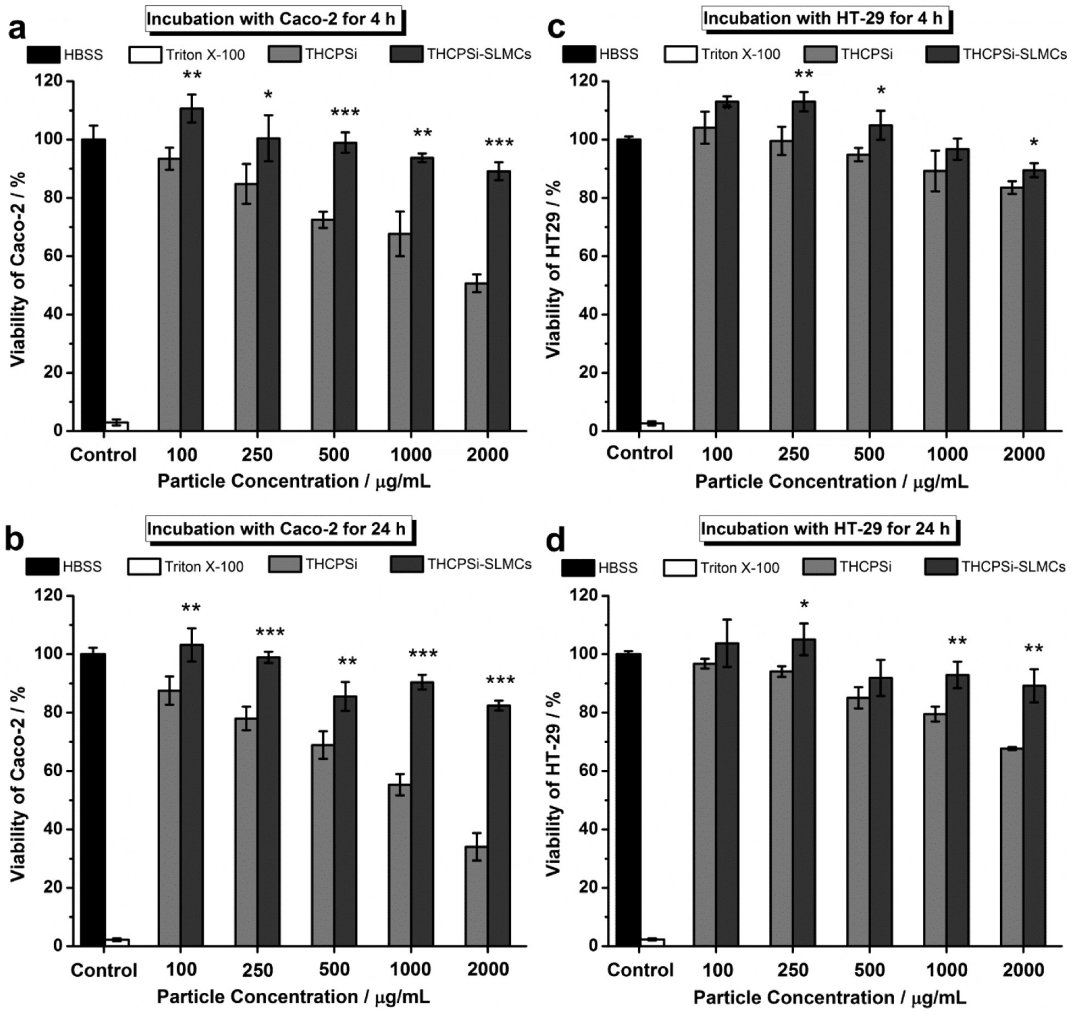

Figure 3. Cell viability of Caco-2 (a, b) and HT-29 (c, d) cancer cells after 4 (a, c) and 24 h (b, d) incubation with different concentrations (μg/mL) of the THCPSi microparticles and THCPSi–SLMCs (calculated on the basis of the amount of PSi particles) assessed by a luminescence-based assay. All experiments were conducted at 37 °C. Errors bars represent the mean ± SD ($n = 4$). The level of significance was set at probabilities of $^{*}p < 0.05$, $^{**}p < 0.01$, and $^{***}p < 0.001$.

loaded using a solution that consisted of a mixture of ethanol and water (50:50, v/v).

The degrees of loading for the four model drugs into the PSi microparticles and into the final microcomposites are listed in Figure 4. For the bare PSi microparticles, the drug-loading degrees varied from about 9% for ranitidine to approximately 25% for furosemide. These differences can be partially ascribed to the different chemical structures and the different solubility characteristics of the two drugs. The ability of the different loading solutions to wet the surface and pores of the PSi microparticles might also have contributed to the variation in the degree of drug loaded.

For the microcomposites, we measured drug-loading degrees that were smaller than those measured for the bare PSi microparticles. This can be attributed to the inevitable partial prerelease of the drugs after exposing the drug-loaded PSi microparticles to the organic solvent during the microfluidic templation of the microcomposites. This decrease was more significant for fenofibrate and furosemide, for which approximately half was prereleased during the templation. In stark contrast, for methotrexate and ranitidine only minute amounts were prereleased during the encapsulation process. These differences were due to the different solubility of the drugs in

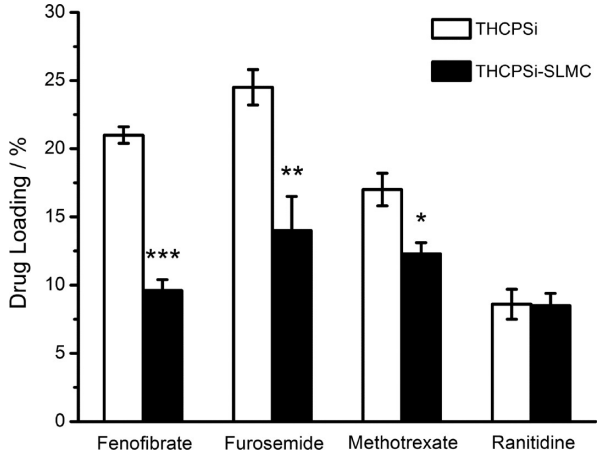

Figure 4. Drug-loading degree (%) for the THCPSi microparticles obtained by the immersion method and THCPSi–SLMCs after microfluidics fabrication (calculated on the basis of the amount of PSi particles). The level of significance was set at probabilities of $^{*}p < 0.05$, $^{**}p < 0.01$, and $^{***}p < 0.001$.

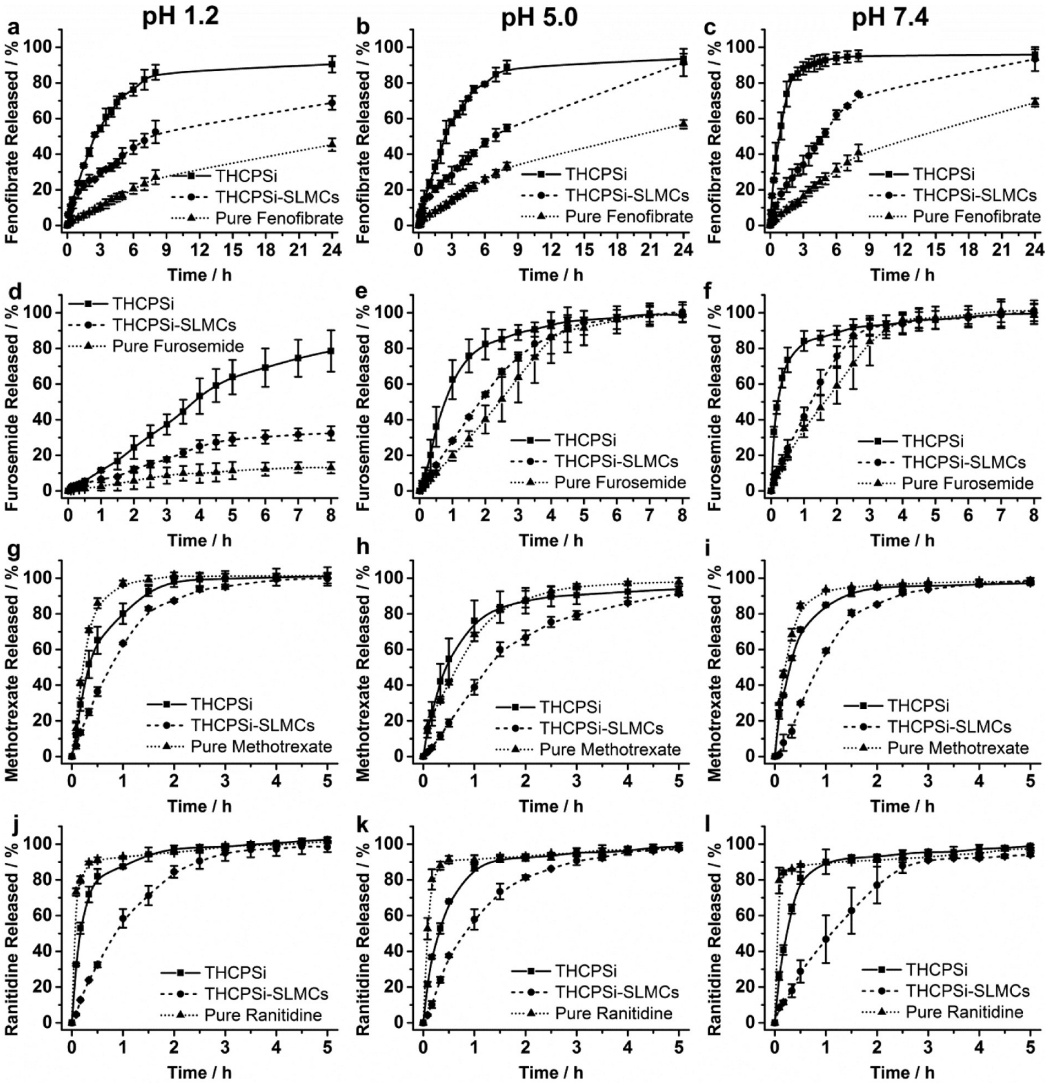

Figure 5. Release profiles of the payloads from THCPSi microparticles and THCPSi−SLMCs. Fenofibrate (a−c), furosemide (d−f), methotrexate (g−i), and ranitidine (j−l) were loaded into the particles, and the release profiles were measured at pH 1.2 (a, d, g, and j), 5.0 (b, e, h, and k), and 7.4 (c, f, i, and l). The dissolution profiles of pure drugs are also shown for comparison. All experiments were conducted at 37 °C. Error bars represent the mean ± SD (n = 3).

the organic inner fluid, ethyl acetate, which was relatively high for fenofibrate and furosemide but moderately low for methotrexate and ranitidine. These results indicate that a poor solubility of the drug in the solvent used as inner fluid in the microfluidic setup is critical to achieve a relatively high degree of drug loading into the PSi microparticles encapsulated within the SLMs. Despite the smaller drug-loading capacity of the microcomposites as compared to that of the bare PSi microparticles, the variation among the different drugs tested was smaller than for the bare PSi microparticles. In addition, the resultant microcomposites allowed the incorporation of rather aqueous-soluble drugs in their structure; these types of drugs are difficult to be loaded into traditional colloids, such as polymeric particles, oil-in-water emulsions, or micelles, because of the inherent hydrophobicity of these matrices.[50−52]

In general, the solubility of the drug in the medium where it must be delivered plays an important role, mainly in determining the time scale of the release process. Aqueous-soluble drugs are typically released faster and with a more significant burst-release effect than poorly aqueous-soluble ones.[49] To test the potential of our microfluidic-templated microcomposites to sustain the release of the payloads and to reduce the initial burst-release effect, particularly for the aqueous-soluble drugs, we measured the release profiles for the four model drugs with different aqueous solubilities loaded within the bare PSi microparticles or in the resultant microcomposites, as shown in Figure 5. We used buffer solutions with pH values of 1.2, 5.0, and 7.4 to simulate the different physiological conditions of the GIT. Among the four model drugs, only fenofibrate and furosemide showed noticeable pH-dependent release profiles. The dissolution of pure fenofibrate and the release rate of fenofibrate from the PSi microparticles or THCPSi−SLMCs were increased gradually with pH, as shown in Figure 5a−c. The release rate of furosemide showed similar trends to those of fenofibrate except for the sharp enhancement that was measured as the pH value was increased from 1.2 to 5.0, as shown in Figure 5d,f. The pH-dependent release profiles for fenofibrate and furosemide from the PSi microparticles and THCPSi−SLMCs could be partly ascribed to the lower solubility of the payloads at lower pH conditions. Furthermore, the significantly different properties of the phospholipid under acidic pH conditions (<3), such as the increased phase-transition temperature, gel-phase characteristics,

and slight alteration of the phospholipid surface charge, could also contribute to the more pronounced slow release rate of the payloads from THCPSi–SLMCs under acidic pH conditions.[53,54] For methotrexate and ranitidine, the impact of the pH on the release profiles was less pronounced than for fenofibrate and furosemide, as shown in Figure 5g–l. For methotrexate, the release rate was only slightly slower at pH 5.0, whereas the release rate of ranitidine was independent of pH for the pH values tested.

Regardless of the pH of the media and the solubility of the four model drugs, the release rate of payloads from the microcomposites was always slower than that from the bare PSi microparticles. For example, in the case of fenofibrate at pH 1.2, the time for the release of 50% fenofibrate from the THCPSi microparticles was about 2.5 h, whereas for the microcomposite it was approximately 7.5 h. This is summarized in Figure 6. More importantly, these microcomposites efficiently reduced the initial burst-release effect of the drugs observed in the case of the bare PSi microparticles, which was more pronounced for the aqueous-soluble drugs. For example, approximately 20% of ranitidine was released from the bare PSi microparticles within the first 5 min, whereas only approximately 5% was released from the corresponding microcomposites, independently of the pH value tested.

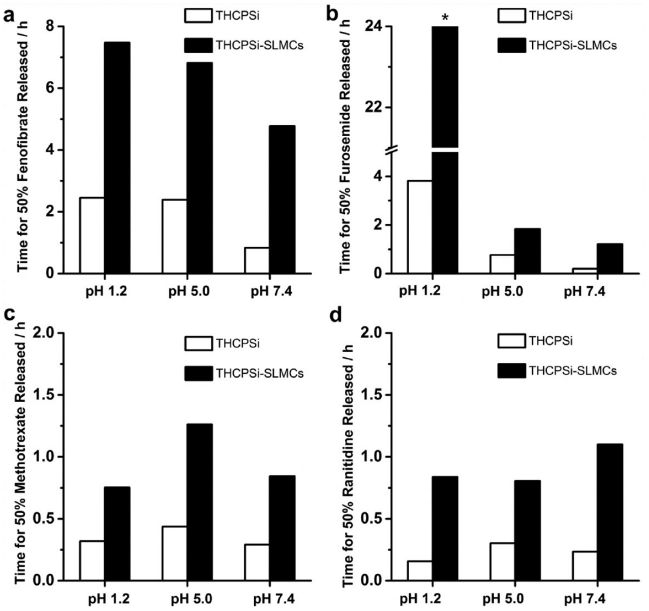

Figure 6. Time for 50% payload released from THCPSi microparticles and THCPSi–SLMCs: (a) fenofibrate, (b) furosemide, (c) methotrexate, and (d) ranitidine. The asterisk (*) represents a release time of more than 24 h.

Therefore, better control over the release of the drugs was achieved with the microcomposites than with the bare THCPSi microparticles. The encapsulation of the bare PSi microparticles within the SLM significantly reduced not only the in vitro release rate of the payloads as compared to that of the bare PSi microparticles but also the initial burst-release effect, which was more pronounced for aqueous-soluble drugs. These properties make the microcomposites excellent candidates for controlled release of drugs, particularly for prolonged drug release with a reduced initial burst-release effect.

4. CONCLUSIONS

Herein, we report a novel approach for the continuous production of monodisperse microcomposites that have potential applications for the sustained release of both hydrophilic and hydrophobic drugs. The microcomposite consisted of drug-loaded PSi microparticles that were efficiently embedded within a SLM. The introduction of the SLM not only rendered the surface of the PSi microparticles less hydrophobic but also yielded microcomposites with uniform morphology and lower cytotoxicity. Moreover, these microcomposites greatly reduced the initial burst-release effect observed when the same drugs were released from the bare PSi microparticles. Overall, this is the first proof of principle that microfluidic approaches can be used to fabricate advanced DDSs based on monodisperse THCPSi–SLMCs for the sustained release of both hydrophobic and hydrophilic drugs, providing a promising platform for controlled drug-delivery applications.

■ ASSOCIATED CONTENT

Ⓢ Supporting Information

HPLC experimental conditions, structures and physicochemical properties details of the model drugs used, and formulation optimization. This material is available free of charge via the Internet at http://pubs.acs.org.

■ AUTHOR INFORMATION

Corresponding Author

*Tel.: +358 9 191 59661; Fax: +358 9 191 59144; E-mail: helder.santos@helsinki.fi.

Author Contributions

⊥These authors contributed equally to this work. The manuscript was written through contributions of all authors. All authors have given approval to the final version of the manuscript.

Notes

The authors declare no competing financial interest.

■ ACKNOWLEDGMENTS

Dr. H. A. Santos acknowledges financial support from the Academy of Finland (decision nos. 252215 and 256394), the University of Helsinki, and the European Research Council under the European Union's Seventh Framework Programme (FP/2007-2013, grant no. 310892).

■ REFERENCES

(1) LaVan, D. A.; McGuire, T.; Langer, R. *Nat. Biotechnol.* **2003**, *21*, 1184–1191.
(2) Santos, H. A. *Biomatter* **2012**, *2*, 237–238.
(3) Langer, R. *Nature* **1998**, *392*, 5–10.
(4) Allen, T. M.; Cullis, P. R. *Science* **2004**, *303*, 1818–1822.
(5) Santos, H. A.; Hirvonen, J. *Nanomedicine* **2012**, *7*, 1281–1284.
(6) Santos, H. A.; Bimbo, L. M.; Lehto, V. P.; Airaksinen, A. J.; Salonen, J.; Hirvonen, J. *Curr. Drug Discov. Technol.* **2011**, *8*, 228–249.
(7) Anglin, E. J.; Cheng, L. Y.; Freeman, W. R.; Sailor, M. J. *Adv. Drug Deliv. Rev.* **2008**, *60*, 1266–1277.
(8) Jaganathan, H.; Godin, B. *Adv. Drug Deliv. Rev.* **2012**, *64*, 1800–1819.
(9) Bimbo, L. M.; Denisova, O. V.; Mäkilä, E.; Kaasalainen, M.; De Brabander, J. K.; Hirvonen, J.; Salonen, J.; Kakkola, L.; Kainov, D.; Santos, H. A. *ACS Nano* **2013**, *7*, 6884–6893.
(10) Kinnari, P. J.; Hyvonen, M. L.; Mäkilä, E. M.; Kaasalainen, M. H.; Rivinoja, A.; Salonen, J. J.; Hirvonen, J. T.; Laakkonen, P. M.; Santos, H. A. *Biomaterials* **2013**, *34*, 9134–9141.

(11) Liu, D.; Bimbo, L. M.; Mäkilä, E.; Villanova, F.; Kaasalainen, M.; Herranz-Blanco, B.; Caramella, C. M.; Lehto, V. P.; Salonen, J.; Herzig, K. H.; Hirvonen, J.; Santos, H. A. *J. Control. Release* **2013**, *170*, 268−278.
(12) Tasciotti, E.; Liu, X. W.; Bhavane, R.; Plant, K.; Leonard, A. D.; Price, B. K.; Cheng, M. M. C.; Decuzzi, P.; Tour, J. M.; Robertson, F.; Ferrari, M. *Nat. Nanotechnol.* **2008**, *3*, 151−157.
(13) Sarparanta, M.; Mäkilä, E.; Heikkila, T.; Salonen, J.; Kukk, E.; Lehto, V. P.; Santos, H. A.; Hirvonen, J.; Airaksinen, A. J. *Mol. Pharmaceutics* **2011**, *8*, 1799−1806.
(14) Bimbo, L. M.; Sarparanta, M.; Santos, H. A.; Airaksinen, A. J.; Mäkilä, E.; Laaksonen, T.; Peltonen, L.; Lehto, V. P.; Hirvonen, J.; Salonen, J. *ACS Nano* **2010**, *4*, 3023−3032.
(15) Low, S. P.; Voelcker, N. H.; Canham, L. T.; Williams, K. A. *Biomaterials* **2009**, *30*, 2873−2880.
(16) Rosengren, A.; Wallman, L.; Bengtsson, M.; Laurell, T.; Danielsen, N.; Bjursten, L. M. *Phys. Status Solidi A* **2000**, *182*, 527−531.
(17) Tanaka, T.; Godin, B.; Bhavane, R.; Nieves-Alicea, R.; Gu, J.; Liu, X.; Chiappini, C.; Fakhoury, J. R.; Amra, S.; Ewing, A.; Li, Q.; Fidler, I. J.; Ferrari, M. *Int. J. Pharm.* **2010**, *402*, 190−197.
(18) Park, J. H.; Gu, L.; von Maltzahn, G.; Ruoslahti, E.; Bhatia, S. N.; Sailor, M. J. *Nat. Mater.* **2009**, *8*, 331−336.
(19) Godin, B.; Gu, J. H.; Serda, R. E.; Bhavane, R.; Tasciotti, E.; Chiappini, C.; Liu, X. W.; Tanaka, T.; Decuzzi, P.; Ferrari, M. *J. Biomed. Mater. Res., Part A* **2010**, *94*, 1236−1243.
(20) Canham, L. T.; Reeves, C. L.; Newey, J. P.; Houlton, M. R.; Cox, T. I.; Buriak, J. M.; Stewart, M. P. *Adv. Mater.* **1999**, *11*, 1505−1507.
(21) Shahbazi, M. A.; Hamidi, M.; Mäkilä, E. M.; Zhang, H.; Almeida, P. V.; Kaasalainen, M.; Salonen, J. J.; Hirvonen, J. T.; Santos, H. A. *Biomaterials* **2013**, *34*, 7776−7789.
(22) Liu, J.; Jiang, X.; Ashley, C.; Brinker, C. J. *J. Am. Chem. Soc.* **2009**, *131*, 7567−7569.
(23) Ashley, C. E.; Carnes, E. C.; Phillips, G. K.; Padilla, D.; Durfee, P. N.; Brown, P. A.; Hanna, T. N.; Liu, J.; Phillips, B.; Carter, M. B.; Carroll, N. J.; Jiang, X.; Dunphy, D. R.; Willman, C. L.; Petsev, D. N.; Evans, D. G.; Parikh, A. N.; Chackerian, B.; Wharton, W.; Peabody, D. S.; Brinker, C. J. *Nat. Mater.* **2011**, *10*, 389−397.
(24) Vallet-Regi, M.; Balas, F.; Arcos, D. *Angew. Chem., Int. Ed.* **2007**, *46*, 7548−7558.
(25) Liu, D.; Mäkilä, E.; Zhang, H.; Herranz, B.; Kaasalainen, M.; Kinnari, P.; Salonen, J.; Hirvonen, J.; Santos, H. A. *Adv. Funct. Mater.* **2013**, *23*, 1893−1902.
(26) Fan, D. M.; De Rosa, E.; Murphy, M. B.; Peng, Y.; Smid, C. A.; Chiappini, C.; Liu, X. W.; Simmons, P.; Weiner, B. K.; Ferrari, M.; Tasciotti, E. *Adv. Funct. Mater.* **2012**, *22*, 282−293.
(27) Bondi, M. L.; Craparo, E. F. *Expert Opin. Drug Delivery* **2010**, *7*, 7−18.
(28) Duncanson, W. J.; Lin, T.; Abate, A. R.; Seiffert, S.; Shah, R. K.; Weitz, D. A. *Lab Chip* **2012**, *12*, 2135−2145.
(29) Xu, Q. B.; Hashimoto, M.; Dang, T. T.; Hoare, T.; Kohane, D. S.; Whitesides, G. M.; Langer, R.; Anderson, D. G. *Small* **2009**, *5*, 1575−1581.
(30) Yang, S.; Guo, F.; Kiraly, B.; Mao, X.; Lu, M.; Leong, K. W.; Huang, T. J. *Lab Chip* **2012**, *12*, 2097−2102.
(31) Capretto, L.; Mazzitelli, S.; Nastruzzi, C. *J. Control. Release* **2012**, *160*, 409−417.
(32) Zhao, Y. J.; Shum, H. C.; Chen, H. S.; Adams, L. L. A.; Gu, Z. Z.; Weitz, D. A. *J. Am. Chem. Soc.* **2011**, *133*, 8790−8793.
(33) Kim, S. H.; Nam, J.; Kim, J. W.; Kim, D. H.; Han, S. H.; Weitz, D. A. *Lab Chip* **2013**, *13*, 1351−1356.
(34) Amstad, E.; Kim, S. H.; Weitz, D. A. *Angew. Chem., Int. Ed.* **2012**, *51*, 12499−12503.
(35) Valencia, P. M.; Farokhzad, O. C.; Karnik, R.; Langer, R. *Nat. Nanotechnol.* **2012**, *7*, 623−629.
(36) Bimbo, L. M.; Mäkilä, E.; Raula, J.; Laaksonen, T.; Laaksonen, P.; Strommer, K.; Kauppinen, E. I.; Salonen, J.; Linder, M. B.; Hirvonen, J.; Santos, H. A. *Biomaterials* **2011**, *32*, 9089−9099.
(37) Kilpelainen, M.; Riikonen, J.; Vlasova, M. A.; Huotari, A.; Lehto, V. P.; Salonen, J.; Herzig, K. H.; Jarvinen, K. *J. Control. Release* **2009**, *137*, 166−170.
(38) Sarparanta, M. P.; Bimbo, L. M.; Mäkilä, E. M.; Salonen, J. J.; Laaksonen, P. H.; Helariutta, A. M. K.; Linder, M. B.; Hirvonen, J. T.; Laaksonen, T. J.; Santos, H. A.; Airaksinen, A. J. *Biomaterials* **2012**, *33*, 3353−3362.
(39) Brunauer, S.; Emmett, P. H.; Teller, E. *J. Am. Chem. Soc.* **1938**, *60*, 309−319.
(40) Chu, L. Y.; Kim, J. W.; Shah, R. K.; Weitz, D. A. *Adv. Funct. Mater.* **2007**, *17*, 3499−3504.
(41) Rytkonen, J.; Miettinen, R.; Kaasalainen, M.; Lehto, V. P.; Salonen, J.; Narvanen, A. *J. Nanomater.* **2012**, *2012*, 9.
(42) Bimbo, L. M.; Mäkilä, E.; Laaksonen, T.; Lehto, V. P.; Salonen, J.; Hirvonen, J.; Santos, H. A. *Biomaterials* **2011**, *32*, 2625−2633.
(43) Santos, H. A.; Riikonen, J.; Salonen, J.; Mäkilä, E.; Heikkila, T.; Laaksonen, T.; Peltonen, L.; Lehto, V. P.; Hirvonen, J. *Acta Biomater.* **2010**, *6*, 2721−2731.
(44) Verma, A.; Stellacci, F. *Small* **2010**, *6*, 12−21.
(45) Karmali, P. P.; Simberg, D. *Expert Opin. Drug Deliv.* **2011**, *8*, 343−357.
(46) Nel, A. E.; Madler, L.; Velegol, D.; Xia, T.; Hoek, E. M. V.; Somasundaran, P.; Klaessig, F.; Castranova, V.; Thompson, M. *Nat. Mater.* **2009**, *8*, 543−557.
(47) Jiang, W.; Kim, B. Y. S.; Rutka, J. T.; Chan, W. C. W. *Nat. Nanotechnol.* **2008**, *3*, 145−150.
(48) Mahmoudi, M.; Lynch, I.; Ejtehadi, M. R.; Monopoli, M. P.; Bombelli, F. B.; Laurent, S. *Chem. Rev.* **2011**, *111*, 5610−5637.
(49) Salonen, J.; Laitinen, L.; Kaukonen, A. M.; Tuura, J.; Bjorkqvist, M.; Heikkila, T.; Vaha-Heikkila, K.; Hirvonen, J.; Lehto, V. P. *J. Control. Release* **2005**, *108*, 362−374.
(50) Liu, D.; Ge, Y.; Tang, Y.; Yuan, Y.; Zhang, Q.; Li, R.; Xu, Q. *J. Microencapsulation* **2010**, *27*, 726−734.
(51) Almeida, A. J.; Souto, E. *Adv. Drug Deliv. Rev.* **2007**, *59*, 478−490.
(52) Liu, D. F.; Jiang, S. M.; Shen, H.; Qin, S.; Liu, J. J.; Zhang, Q.; Li, R.; Xu, Q. W. *J. Nanopart. Res.* **2011**, *13*, 2375−2386.
(53) Zhou, Y.; Raphael, R. M. *Biophys. J.* **2007**, *92*, 2451−2462.
(54) Trauble, H.; Eibl, H. *Proc. Natl. Acad. Sci. U.S.A.* **1974**, *71*, 214−219.